

NUMERICAL INVESTIGATION OF COUPLED NATURAL CONVECTION AND SURFACE RADIATION IN A SQUARE CAVITY WITH THE LINEARLY HEATED SIDE WALL(S)

Ravi Shankar Prasad^{a,*}, S.N. Singh^b, Amit Kumar Gupta^c

^a Department of Mechanical Engineering, B.I.T. Sindri, Dhanbad, Jharkhand, PIN 828123, India

^b Department of Mechanical Engineering, Indian Institute of Technology (Indian School of Mines), Dhanbad, Jharkhand, PIN 826004, India

^c Department of Chemical Engineering, B.I.T. Sindri, Dhanbad, Jharkhand, PIN 828123, India

ABSTRACT

The results of numerical analysis of coupled laminar natural convection and surface radiation in a two-dimensional closed square cavity with the uniformly heated bottom wall, linearly heated vertical side wall(s) and the adiabatic top wall is discussed. The cavity is filled with natural air ($Pr = 0.70$) as the fluid medium. In the present study, the governing equations i.e., the Navier-Stokes Equation in the stream function – vorticity form and the Energy Equation are solved for a constant property fluid under the Boussinesq approximation. For discretization of these equations, the finite volume technique is used. For the radiation calculations, the radiosity-irradiation formulation is used and the shape factors are calculated by using the Hottel's crossed-string method. The effects of pertinent parameters like the Rayleigh Number ($10^3 \leq Ra \leq 10^6$) and the surface emissivity of walls ($0.05 \leq \varepsilon \leq 0.85$) are analyzed.

Keywords: closed cavity, free convection, linearly heated, radiation, stream function, vorticity

1. INTRODUCTION

Natural convection in the closed and open cavities has received a wide and renewed attention by the researchers and industrial scientists in the recent years. The prime reasons attributed for it underlies in its important role in many engineering and practical science applications like power plant engineering, cooling of electrical generators, solar energy, etc. Some of the other important applications of natural convection are effective cooling of internal combustion engines, air conditioning and refrigeration, aerospace engineering, cryogenics, safe design of nuclear reactors, fire control engineering, chemical and biological warfare, chemical and metallurgical engineering, food processing industries, meteorological predictions, ocean engineering, etc. The natural convection is the prime consideration in the design of building ventilation as well as natural ventilation in mines and tunnels.

The nuclear reactor accident at Fukushima in 2011 was caused due to failure of the pump of cooling system. The cooling system of next generation nuclear reactors are expected to remain functional even when the pump is not working. Natural convection can be used to flow the coolant without using a pump (Abdillah and Novitrian, 2019). One of the prime criteria for safe design of an electronic equipment is its cooling performance by unaided natural convection. For heat dissipation and cooling, natural convection is preferred because of its inherent simplicity, reliability, quite operation and economy.

In the most of such problems, the heat sources are assumed either having a constant temperature or generating heat at a constant rate for the sake of simplicity and convenience. This is an idealistic approach from the practical point of view. In most of the practical cases, the heat sources may have varying temperature with the different temperature profiles.

The linearly varying temperature is one of the cases, which resembles a very close approximation to the several practical situations. One of such practical situations is one side of wall being heated or cooled by a water jacket, which contains the coldest water at bottom and the hottest water at top. An example of wall having varying temperature is a heat generating wall with the varying insulation thickness. A heat generating wall of varying thickness from bottom to top may also form a wall of varying temperature. Studying the effect of linearly varying temperature and other parameters on natural convection coupled with surface radiation in a closed cavity is one of the realistic problems of broad practical importance. Such a problem of cooling by natural convection coupled with surface radiation needs to be investigated and analyzed for the better understanding of its mechanism.

Ostrach (1954) presented an extensive study of combined natural and forced convection laminar flow and heat transfer of fluids with and without the heat sources in the channels with the linearly varying wall temperatures. Jones and Ingham (1993) studied the combined convection flow in a vertical duct with linearly varying wall temperatures with depth. Balaji and Venkateshan (1994a) derived the correlations for the free convection and surface radiation in a square cavity. Balaji and Venkateshan (1994b) studied the interaction of radiation with the free convection in an open cavity. These research works by Balaji and Venkateshan (1994a and 1994b) discusses the effect of surface radiation on natural convection inside the cavities. The correlations are developed for the convective and the radiative heat transfer on the basis of numerical results.

Singh and Venkateshan (2004) made a numerical study of natural convection with surface radiation in side-vented open cavities. It is found that the surface radiation affects the basic flow pattern and isotherms inside the cavity significantly. The thermal boundary layers along the

* Corresponding author. Email: rsprasad.me@bitsindri.ac.in

adiabatic walls of the cavity are found as a result of the interaction of natural convection and surface radiation. Prud'homme and Bougherara (2005) analyzed the weak non-linear stability of stratified natural convection in a vertical cavity with lateral temperature gradient. Sathiyamoorthy *et al.* (2007a) studied the effect of the temperature difference aspect ratio on natural convection in a square cavity for nonuniform thermal boundary conditions. Sathiyamoorthy *et al.* (2007b) performed a numerical investigation of steady natural convection flows in a square cavity with the linearly heated side wall(s). Sathiyamoorthy *et al.* (2007c) studied the steady natural convection flow in a square cavity filled with a porous medium for the linearly heated side wall(s). The research works by Sathiyamoorthy *et al.* (2007a, 2007b and 2007c) discusses the pure natural convection inside the cavities having the linearly heated side walls.

Bouafia and Daube (2007) studied the natural convection for large temperature gradients around a square solid body within a rectangular cavity. Natarajan *et al.* (2007) studied natural convection in a trapezoidal cavity with linearly heated side wall(s). Basak *et al.* (2009a) made an analysis of mixed convection flows within a square cavity with linearly heated side wall(s). Basak *et al.* (2009b) made a natural convection flow simulation for various angles in a trapezoidal enclosure with the linearly heated side wall(s). Basak *et al.* (2010) analyzed the mixed convection in a lid-driven porous square cavity with linearly heated side wall(s). Sathiyamoorthy and Chamkha (2010) studied the effect of the externally imposed magnetic field inclined at an angle ϕ with respect to the horizontal plane on natural convection flow in an electrically conducting liquid gallium filled square cavity having linearly heated side wall(s).

Al-Salem *et al.* (2012) studied the effects of moving lid direction on MHD mixed convection in a linearly heated cavity. Hasan *et al.* (2012) investigated the unsteady natural convection within a differentially heated enclosure of sinusoidal corrugated side walls. Kefayati *et al.* (2012) made a Lattice Boltzmann simulation of MHD mixed convection in a lid-driven square cavity with linearly heated wall. Sathiyamoorthy and Chamkha (2012) investigated the natural convection flow under magnetic field in a square cavity for the uniformly and the linearly heated adjacent walls. It is observed that the presence of a magnetic field has significant effects on the local and average Nusselt numbers on walls. Kefayati (2014) analyzed the natural convection of ferrofluid in a linearly heated cavity utilizing Lattice Boltzmann method. The cavity is filled with the kerosene as the carrier fluid and the nanoscale ferromagnetic particle of cobalt. The influence of the external magnetic source on the nanoscale ferromagnetic particle at the different Rayleigh number is studied. Basak *et al.* (2013) studied the effect of various orientations on natural convection in tilted isosceles triangular enclosures with the linearly heated inclined walls. Saravanan and Sivaraj (2015) reported the results of the combined natural convection and thermal radiation in a square cavity with a non-uniformly heated plate. It is found that the heat transfer rate for a vertically placed plate is always significantly higher than that of a horizontally oriented one. Singh and Singh (2015) performed a numerical investigation of conjugate free convection with surface radiation in an open top cavity. It is found that the locations of heat source have a significant effect on the fluid flow and heat transfer inside the cavity. The best position of heat source for its cooling is at the top of the left side wall inside the cavity.

Mahmoodi *et al.* (2017) performed a numerical study of natural convection in nanofluid filled square chambers subjected to linear heating on both sides. The maximum and minimum local Nusselt number at the ends of the left wall and heat transfer increases with increase in the Rayleigh number and the volume fraction of the nanoparticles. Karatas and Derbentli (2018) analyzed natural convection and radiation in rectangular cavities with one active vertical wall. The variations of temperature and local Nusselt number along the cavity height is presented. Prasad *et al.* (2018a) proposed a systematic approach for optimal positioning of heated side walls in a side vented open cavity under natural convection and surface radiation. Prasad *et al.* (2018b) analyzed coupled laminar natural convection and surface radiation in

partially right side open cavities. Sankar *et al.* (2018) analyzed the natural convection in a linearly heated vertical porous annulus. Chaabane (2019) analyzed the free convection in a MHD open cavity with a linearly heated wall using Lattice Boltzmann method. Prasad *et al.* (2019) studied the combined laminar natural convection and surface radiation in top open cavities with right side opening. The research works by Prasad *et al.* (2018a, 2018b and 2019) presents the numerical investigation of coupled natural convection and surface radiation inside the open cavities with the purpose of optimization of cooling of heat sources inside the cavities. These research papers present the effect of surface radiation on natural convection in open cavities. Mliki *et al.* (2020) made a Lattice Boltzmann simulation of MHD natural convection heat transfer of Cu-water nanofluid in the linearly and the sinusoidally heated cavities. Şahin (2020) studied the effects of the center of linear heating position on natural convection and entropy generation in a linearly heated square cavity. It is observed that the position of the center of linear heating has a substantial effect on entropy generation and heat transfer by natural convection. It is further shown that as the center of linear heating is shifted upwards, the fluid flow is moved to the right.

Kiran *et al.* (2021) studied natural convection in a linearly heated vertical porous annulus under the effect of magnetic field. It is found that the magnetic force plays a prime role in delaying the buoyant flow and the resultant thermal transport in the annulus. Kumar and Kunjuni (2021) studied the effect of linearly varying heating inside a square cavity under natural convection. Prasad *et al.* (2022) made a numerical investigation of combined natural convection and surface radiation in a square cavity with the inversely linearly heated opposite side walls. The streamlines and isotherms at different Rayleigh numbers is presented.

Natural convection in the cavities having linearly heated sidewall(s) has been studied by only a few researchers. Due to lack of experimental data available for the such cavities, the results presented earlier by the other researchers need to be compared with the results of these cavities using other approaches and mathematical formulations to establish the validity of these results. Sathiyamoorthy *et al.* (2007b) performed a numerical investigation of steady natural convection flows in a square cavity with the linearly heated side wall(s). Sathiyamoorthy *et al.* (2007b) solved the governing equations in the primitive variables using the Galerkin finite element method. In the present study, the stream function-vorticity formulation is used for natural convection and the governing equations are solved by using the finite volume based finite difference method. In the study by Sathiyamoorthy *et al.* (2007b), the heat transfer between the cavity walls by thermal radiation is completely ignored. But even at the moderate emissivity of the cavity walls, the heat transfer by the thermal radiation is significant and affects the natural convection inside the cavity. Thus, the results presented by Sathiyamoorthy *et al.* (2007b) need to be compared and revised by considering the thermal radiation heat transfer between the cavity walls.

Further, it is also noted that none of the researchers have analyzed the coupled natural convection with the surface radiation in a cavity with the linearly heated sidewall(s). This paper fills this research gap by studying natural convection in conjunction with the surface radiation in a cavity having the linearly heated side walls.

Analysis of different types of temperature distribution and different heat sources provides an insight to understand the mechanism of natural convection in a better convincing way. This is helpful in analyzing the different practical situations arising with a number of heat sources or extended heat source with the varying temperature in a confined area. This is useful in the optimization of cooling of different heat sources for the compact design of the devices having such heat generating components.

2. MATHEMATICAL FORMULATION

The mathematical formulation used for natural convection and surface radiation, computational domain as well as the boundary conditions used is presented here.

2.1 Formulation for Natural Convection

The two-dimensional steady incompressible laminar natural convection heat transfer in a closed rectangular cavity having height 'H' and horizontal width 'd' (= H) is considered. Here, the Cartesian co-ordinate system is used as shown in Fig. 1.

The governing equations in stream function (ψ) - vorticity (ω) form for a constant property fluid under the Boussinesq approximation, in the non-dimensional form are:

$$U \frac{\partial \omega}{\partial X} + V \frac{\partial \omega}{\partial Y} = Pr. \left[\frac{\partial^2 \omega}{\partial X^2} + \frac{\partial^2 \omega}{\partial Y^2} \right] - Ra. \frac{\partial \theta}{\partial Y} \quad (1)$$

$$\frac{\partial^2 \psi}{\partial X^2} + \frac{\partial^2 \psi}{\partial Y^2} = -Pr. \omega \quad (2)$$

$$U \frac{\partial \theta}{\partial X} + V \frac{\partial \theta}{\partial Y} = \frac{\partial^2 \theta}{\partial X^2} + \frac{\partial^2 \theta}{\partial Y^2} \quad (3)$$

where $U = \frac{\partial \psi}{\partial Y}$, $V = -\frac{\partial \psi}{\partial X}$ and $\omega = \frac{\partial V}{\partial X} - \frac{\partial U}{\partial Y}$

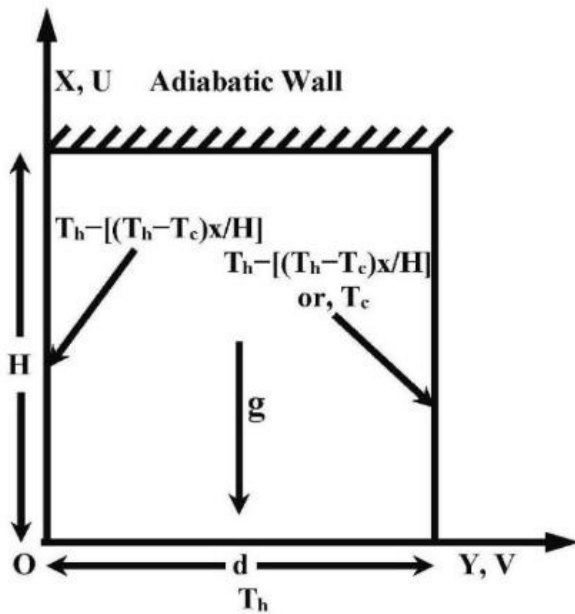


Fig. 1 Schematic diagram of problem geometry showing the computational domain

2.2 Formulation for Surface Radiation

The radiosity-irradiation formulation is used to describe the surface radiation based on Balaji and Venkateshan (1994a and 1994b) and Singh and Venkateshan (2004). The walls are assumed to be diffuse and gray i.e., independent of direction and wavelength. For an elemental area on the boundary of the cavity, the non-dimensional radiosity is given by the following equation.

$$J_i = \varepsilon_i (T_i/T_h)^4 + (1 - \varepsilon_i) \sum_{j=1}^{2(m+n-2)} F_{ij} J_j \quad (4)$$

where $i = 1, 2(m+n-2)$.

Here the view factors F_{ij} are calculated using the Hottel's crossed string method.

2.3 Boundary Conditions

The boundary conditions for the computational domain enclosed by the cavity are specified in terms of non-dimensional stream function, vorticity and temperature based on the Balaji and Venkateshan (1994a and 1994b), Singh and Venkateshan (2004) and Sathiyamoorthy *et al.* (2007b). The boundary conditions are written in terms of the velocities U and V also for the clarity and simplicity only.

2.3.1 Boundary condition for left side linearly heated wall

For the case of left side linearly heated wall:

$$T_x = T_h - [(T_h - T_c)x/H] \quad (5)$$

$$\text{Hence, } \theta = \frac{T_x - T_c}{T_h - T_c} = 1 - \frac{x}{H} = 1 - \frac{x}{d} = 1 - X \quad (6)$$

[Since for a square cavity, $A = 1$, $H = d$]

Thus, the boundary condition for the left side linearly heated wall is,

$$0 < X < A, \quad Y = 0, \quad U = 0, V = 0, \text{ or } \psi = 0,$$

$$\omega = -\frac{1}{Pr} \frac{\partial^2 \psi}{\partial Y^2}, \quad \theta = 1 - X \quad (7)$$

2.3.2 Boundary condition for bottom isothermal wall

At the bottom isothermal wall, $T = T_h$ or, $\theta = 1$

Thus, the boundary condition for the bottom isothermal wall is,

$$X = 0, \quad 0 < Y < I, \quad U = 0, V = 0, \text{ or } \psi = 0,$$

$$\omega = -\frac{1}{Pr} \frac{\partial^2 \psi}{\partial X^2}, \quad \theta = 1 \quad (8)$$

2.3.3 Boundary condition for right side wall

The boundary condition for the right side linearly heated wall is,

$$0 < X < A, \quad Y = I, \quad U = 0, V = 0, \text{ or } \psi = 0,$$

$$\omega = -\frac{1}{Pr} \frac{\partial^2 \psi}{\partial Y^2}, \quad \theta = 1 - X \quad (9)$$

For the case the right side wall is a cold wall, the boundary condition for the right side wall is,

$$0 < X < A, \quad Y = I, \quad U = 0, V = 0, \text{ or } \psi = 0,$$

$$\omega = -\frac{1}{Pr} \frac{\partial^2 \psi}{\partial Y^2}, \quad \theta = 0 \quad (10)$$

2.3.4 Boundary condition for top adiabatic wall

At the adiabatic walls, the convection and radiation energy transfer balance each other.

$$\text{Hence, for the top adiabatic wall, } \frac{\partial \theta}{\partial X} = N_{rc}(J - G) \quad (11)$$

Thus, the boundary condition for the top adiabatic wall is,

$$X = A, \quad 0 < Y < I, \quad U = 0, V = 0, \text{ or } \psi = 0,$$

$$\omega = -\frac{1}{Pr} \frac{\partial^2 \psi}{\partial X^2}, \quad \frac{\partial \theta}{\partial X} = N_{rc}(J - G) \quad (12)$$

3. NUMERICAL METHOD AND CHOICE OF PARAMETERS

The governing equations (1), (2) and (3) are transformed into finite difference equations using the finite volume based finite difference method. Then the Gauss-Seidel iterative procedure is used to solve the algebraic equations obtained. The set of discretized equations obtained are solved by using Gauss-Seidel iterative procedure. A computer code for a FORTRAN platform is developed for solving the discretized equations. An optimum grid size of 41x41 is selected for the computational domain on the basis of grid sensitivity analysis as suggested by Singh and Venkateshan (2004). A cosine function has been chosen to generate the grids along both the X and Y directions in the computational domain enclosed by the closed cavity. These cosine grids are very fine near the solid boundaries, where the gradients are very steep, while they are relatively coarser in the remaining part of the domain. A typical cosine grid used is shown in Fig. 2. Derivative boundary conditions are implemented by three points formulae using the Lagrangian polynomial. The integration required in calculations is performed by using the Simpson's one-third rule for the non-uniform step size. Upwinding has been used for representing the advection terms to ensure the stable and convergent solutions. Under relaxation with a

relaxation parameter 0.1 is used for all the equations except for the radiosity equations, where the relaxation parameter 0.5 is used.

A convergence criterion (δ) in the percentage form has been defined as

$$\delta = \left| \frac{\zeta_{new} - \zeta_{old}}{\zeta_{new}} \right| \times 100 \quad (13)$$

where ζ is any dependent variable like ψ , ω , θ , J and G , over which the convergence test is applied. Here the subscripts “old” and “new” refers to the first and second values of ζ calculated in the any two successive iterations. A convergence criterion of 0.1% or 10^{-3} has been used for stream function, vorticity and temperature, whereas the convergence criterion of 0.01% or 10^{-4} has been used for the radiosity.

The Table 1 shows the range of parameters considered in the present study. The results are presented with the objective of analytical comparison between the different cases considered.

Table 1 Range of parameters for the present study

Parameters	Range
Rayleigh Number, Ra_H	10^3 - 10^6
Conduction-radiation parameter, N_{rc}	42.261
Emissivity, ε	0.05-0.85
Temperature ratio, T_R	0.854
Aspect Ratio, A	1.0

3.1 Grid Sensitivity Study

A grid sensitivity study or grid independence study based on \overline{Nu}_C , \overline{Nu}_R and \overline{Nu}_T at the uniformly heated bottom wall is performed to find the optimum grid size as suggested by Singh and Venkateshan (2004). On the basis of this grid independence test a grid size 41x41 is found to be optimum for the present problem.

The change in various parameters like the top wall temperature and the vertical air velocity at the different horizontal sections is not significant with the further increase in the grid size. The validity of optimum grid size with some other relevant parameters is also analyzed. The streamlines and isotherms at different grid sizes is also analyzed, which are not presented here. Any further increase in the grid size increases the computational work manifolds without more significant improvement in the accuracy of the results.

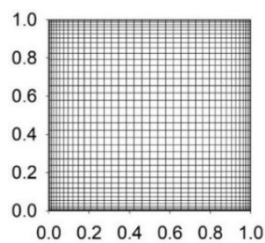


Fig. 2 Typical grid patterns used in the analysis. $A=1$, Grid size = 41×41 .

3.2 Code Validation

There is a lack of experimental results for the cavities having linearly heated side walls in the similar cases and only a few numerical results are available in the similar cases for comparison. For validation, the results obtained using the present code are compared with the numerical results of Sathiyamoorthy *et al.* (2007b). Streamlines and isotherms inside the cavity having left and right side linearly heated side walls under pure natural convection at the different Rayleigh numbers are shown in the Figs. 3 and 4 respectively.

3.2.1 Streamlines inside the cavity under pure natural convection at different Rayleigh numbers using the present code

Fig. 3 presents the streamlines inside the cavity under pure natural convection at different Rayleigh numbers using the present code.

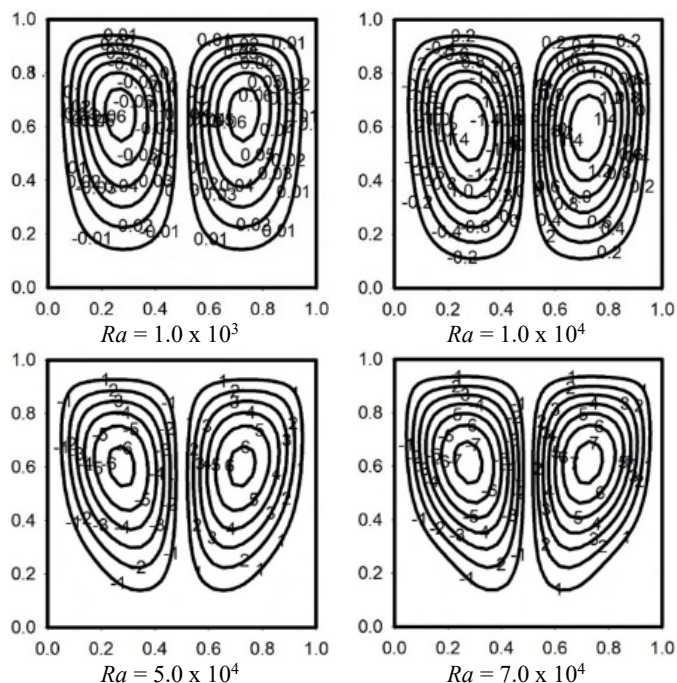


Fig. 3 Streamlines using the present code for the pure natural convection

3.2.2 Isotherms inside the cavity under pure natural convection at different Rayleigh numbers using the present code

Fig. 4 presents the isotherms inside the cavity under pure natural convection at different Rayleigh numbers using the present code.

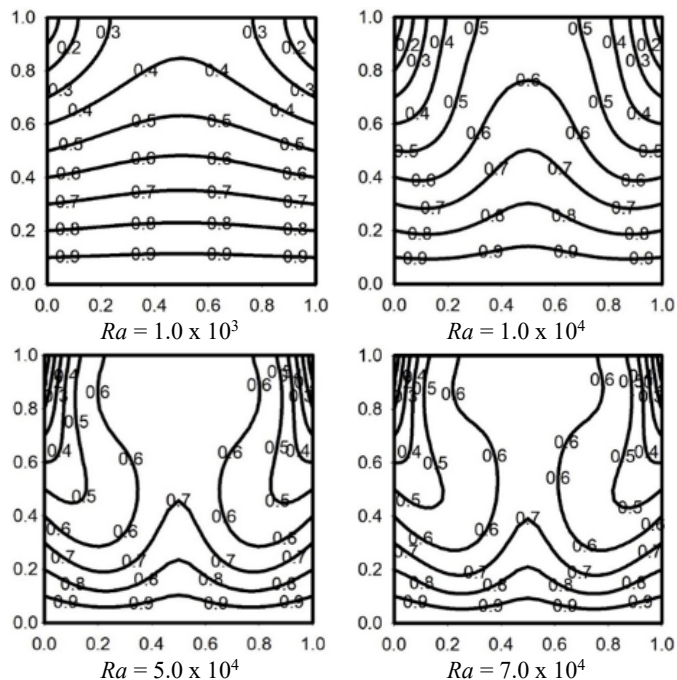


Fig. 4 Isotherms using the present code for the pure natural convection

Fig. 3 and 4 shows the streamlines and isotherms respectively plotted using the present code for the $Ra = 1.0 \times 10^3$, 1.0×10^4 , 5.0×10^4 and 7.0×10^4 .

These streamlines and isotherms at different Rayleigh numbers using the present code are compared with the results of Sathiyamoorthy

et al. (2007b). There a very good agreement is observed between these streamlines and isotherms using the present code and in the results of Sathiyamoorthy *et al.* (2007b).

4. RESULTS AND DISCUSSION

The surface thermal radiation is always inherently present in a heat transfer phenomenon. The surface thermal radiations contribute to the radiative heat transfer between the walls and heating of adiabatic top wall.

In this section, the coupled natural convection with surface thermal radiation in a closed square cavity is discussed. In the first case, the coupled natural convection with surface thermal radiation in a closed square cavity with the uniformly heated bottom wall, identically linearly heated left and right side vertical walls and adiabatic top wall is studied. In the second case, the coupled natural convection with surface thermal radiation in a closed square cavity with the uniformly heated bottom wall, linearly heated left side vertical wall, cold right side vertical wall and adiabatic top wall is analyzed.

Streamlines and isotherms inside the cavity at the different Rayleigh numbers are shown and discussed. Convection Nusselt number (Nu_C) and radiation Nusselt number (Nu_R) at the uniformly heated hot bottom wall and linearly heated vertical side wall(s) at the different Rayleigh numbers are plotted and analyzed.

The results like streamlines, isotherms, variations in Nu_C and Nu_R etc. are discussed in this section and compared with the results of Sathiyamoorthy *et al.* (2007b), where the pure natural convection without surface radiation in cavity is considered. Here several important remarkable observations are made, which indicates the importance of radiative heat transfer in the cavities. This reveals that the radiative heat transfer between the walls of the cavities affects the temperature of the adiabatic wall and hence the natural convection in the cavities. This comparison shows that ignoring the heat transfer by thermal radiation may cause a significant error in the present analysis.

In order to study the importance of the radiative heat transfer, emissivity of all the walls of square cavity is considered high. Here the emissivity of all the walls is considered same and equal to 0.85.

4.1 Analysis of Coupled Natural Convection with Surface Radiation in a Square Cavity having linearly heated left and right side wall

The analysis of coupled natural convection with surface radiation in a square cavity having both left and right side linearly heated wall is presented here.

4.1.1 Variation of Streamlines with Rayleigh Number

In Fig. 5, streamlines are shown for the square cavities having the linearly heated left and right side walls at different Rayleigh numbers ($10^3 \leq Ra \leq 10^6$).

Here, anticlockwise and clockwise air circulations in the cavity are shown via negative and positive signs of stream functions respectively.

It is observed that due to uniformly heated hot bottom wall and linearly heated side walls the hot air rises upwards in the middle part of the cavity and flows downwards along its side walls. Thus, the whole volume of the cavity is divided into two zones, the left zone having an anticlockwise air circulation and the right zone having a clockwise air circulation. These two air circulations form two symmetric rolls in the cavity at the two sides of its central line of symmetry.

At the lower Rayleigh number ($Ra = 1.0 \times 10^3$), the magnitude of stream function is lower showing the weak circulation of air. At the higher Rayleigh numbers, the air circulation becomes stronger at the major part of the cavity. There some minor secondary air circulations may be present at the left and right bottom corners of the cavity.

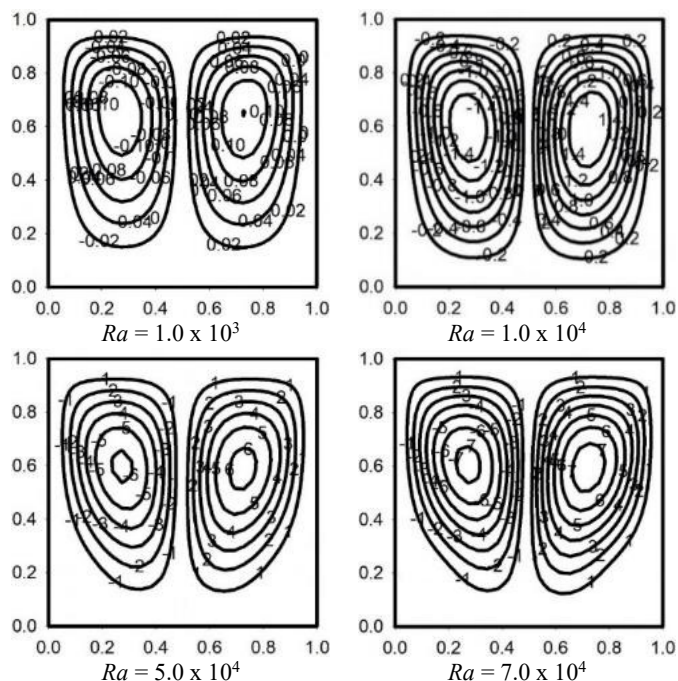


Fig. 5 Variation of streamlines with Rayleigh number (For $A = 1$, $N_{rc} = 42.261$, $Pr = 0.70$, $T_R = 0.854$, $\epsilon = 0.85$)

4.1.2 Variation of Isotherms with Rayleigh Number

In Fig. 6, isotherms are shown for the square cavities with the linearly heated left and right side walls at different Rayleigh numbers ($10^3 \leq Ra \leq 10^6$).

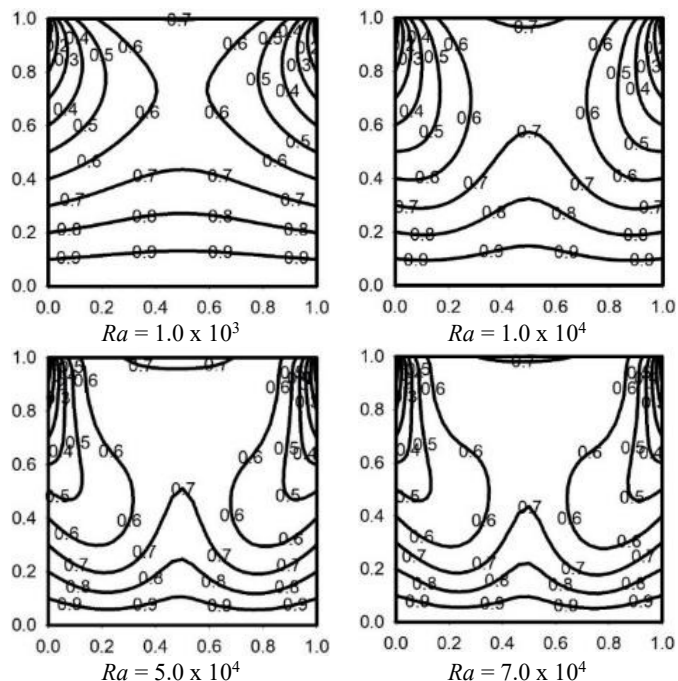


Fig. 6 Variation of isotherms with Rayleigh number (For $A = 1$, $N_{rc} = 42.261$, $Pr = 0.70$, $T_R = 0.854$, $\epsilon = 0.85$)

It is observed that at the lower Rayleigh number ($Ra = 1.0 \times 10^3$), the air circulation in cavity is weak and the conduction dominates. The temperature contours are smooth curves symmetrical about the central line. At the bottom, it extends from left to right as the horizontal parallel lines, whereas at the upper portion the isotherms are bulged upwards.

There is a significant effect of radiative heat transfer on the isotherms. At the lower Rayleigh number, the heat transfer by conduction and radiation dominates, but at the higher Rayleigh number the convective heat transfer increases.

4.1.3 Variation of Local Nu_C at Bottom Wall with Rayleigh Number

In the Fig. 7, the variation of the local Nu_C at the bottom wall with Rayleigh number is shown. At the left and right ends, the local Nu_C is equal to unity due to the linearly heated side walls. In all the cases, the local Nu_C is minimum at the middle. The formation of two symmetric circulations and a weak circulation near the middle of the bottom wall may be attributed to the lower value of local Nu_C at the center of bottom wall. The other factors influencing the local Nu_C at bottom wall are secondary air circulations arising at the left and right bottom corners at higher Rayleigh numbers.

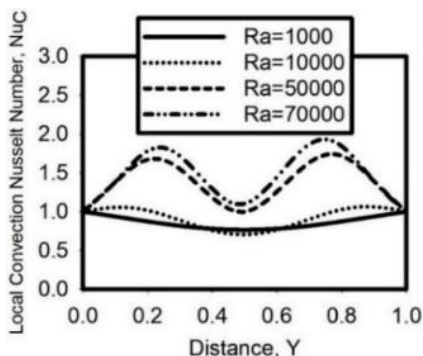


Fig. 7 Variation of local Nu_C at bottom wall with Rayleigh number (For $A = 1$, $N_{rc} = 42.261$, $Pr = 0.70$, $T_R = 0.854$, $\varepsilon = 0.85$)

4.1.4 Variation of Local Nu_R at Bottom Wall with Rayleigh Number

Fig. 8 shows the variation of the local Nu_R at the bottom wall with Rayleigh number. The profile of plot is symmetrical about the central line due to symmetry of problem geometry. The local Nu_R increases continuously from the two sides to the central line and it is highest at the center. This may be attributed to the fact that the central part of the bottom wall is farthest from the all other side walls. Thus, it receives the least amount of irradiation from the other solid walls and the cooling by radiative heat transfer is enhanced. It is observed that with the increase in Rayleigh number, the local Nu_R at bottom wall is slightly reduced.

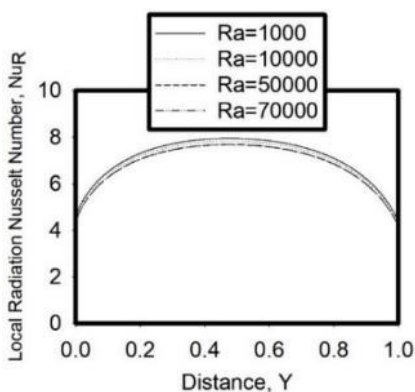


Fig. 8 Variation of local Nu_R at bottom wall with Rayleigh number (For $A = 1$, $N_{rc} = 42.261$, $Pr = 0.70$, $T_R = 0.854$, $\varepsilon = 0.85$)

4.1.5. Variation of Local Nu_C at Linearly Heated Left and Right Side Walls with Rayleigh Number

Fig. 9 shows the variation of the local Nu_C at the linearly heated left and right side walls. It is zero at the bottom due to uniformly heated bottom

wall and hot side walls. It is maximum at the top edge near the adiabatic top wall. Here at the lower Rayleigh number ($Ra = 1.0 \times 10^3$), the local Nu_C at the left and right side walls is close to zero up to a distance $X = 0.6$ due to the weak air circulations. At the higher Rayleigh numbers, the presence of strong air circulation causes increase in the local Nu_C . The local Nu_C is fluctuating at the linearly heated left and right side wall near the bottom wall. This is due to interaction between the downward primary and secondary air circulations with the linearly heated left and right side walls.

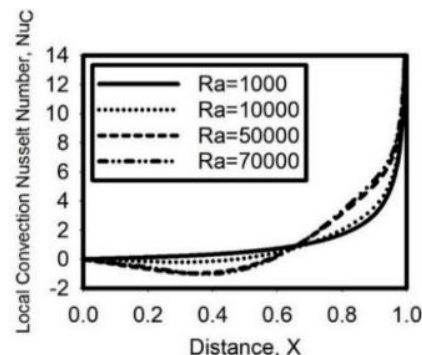


Fig. 9 Variation of local Nu_C at linearly heated left and right side walls with Rayleigh number (For $A = 1$, $N_{rc} = 42.261$, $Pr = 0.7$, $T_R = 0.854$, $\varepsilon = 0.85$)

4.1.6 Variation of Local Nu_R at linearly heated left and right side walls with Rayleigh number

Fig. 10 shows the variation of local Nu_R at the linearly heated left and right side walls. In this plot, the local Nu_R is negative at the bottom of linearly heated vertical side walls and it has a very high positive values near the top wall. The negative value of local Nu_R at the bottom shows that there the left and right side walls are losing heat by radiative heat transfer. The upper part of left and right side walls have a positive local Nu_R showing that there it is gaining heat by radiative heat transfer. Near the top edge, the left and right side walls have a very high positive value of local Nu_R due to presence of the adiabatic top wall close to it.

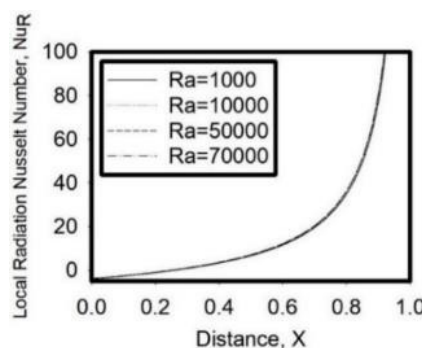


Fig. 10 Variation of local Nu_R at linearly heated left and right side walls with Rayleigh number (For $A = 1$, $N_{rc} = 42.261$, $Pr = 0.70$, $T_R = 0.854$, $\varepsilon = 0.85$)

4.1.7 Variation of $\overline{Nu_C}$ and $\overline{Nu_R}$ at Bottom Wall with Surface Emissivity

Fig. 11 shows the variation of $\overline{Nu_C}$ and $\overline{Nu_R}$ at the bottom surface of cavity with the emissivity of cavity walls.

It can be observed that the $\overline{Nu_C}$ is almost constant with increasing emissivity. This may be attributed to the fact that the emissivity of the side walls has a less significant effect on the cooling by air circulation inside the cavity.

The $\overline{Nu_R}$ at the bottom surface increases linearly with the emissivity of cavity walls. This may be attributed to the fact that radiative heat

transfer between the walls is directly proportional to the emissivity of the cavity walls.

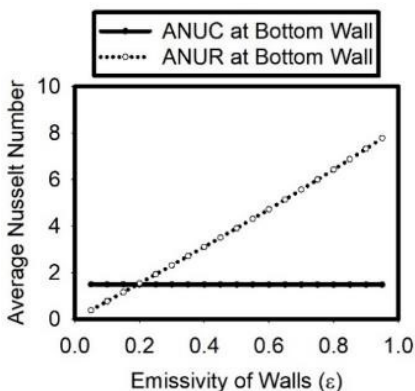


Fig. 11 Variation of \overline{Nu}_C (ANUC) and \overline{Nu}_R (ANUR) at bottom surface with surface emissivity (For $A = 1, N_{rc} = 42.261, Pr = 0.70, Ra = 7.0 \times 10^4, T_R = 0.854$)

4.2 Analysis of Coupled Natural Convection with Surface Radiation in a Square Cavity having linearly heated left side wall and cold right side wall

The analysis of coupled natural convection with surface radiation in a square cavity having left side linearly heated wall and cold right side wall is presented here.

4.2.1 Variation of Streamlines with Rayleigh Number

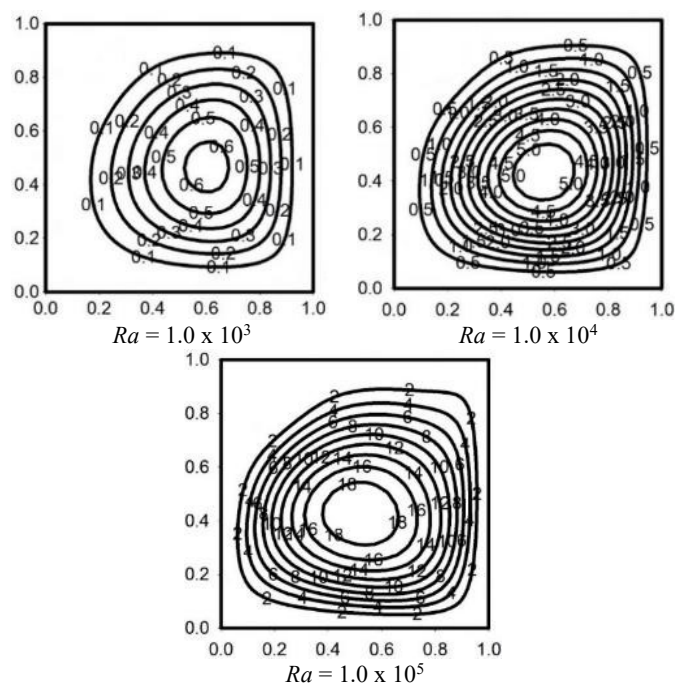


Fig. 12 Variation of streamlines with Rayleigh number (For $A = 1, N_{rc} = 42.261, Pr = 0.70, T_R = 0.854, \epsilon = 0.85$)

Streamlines are shown in Fig. 12 for the square cavities with the linearly heated left side wall and cold right side wall at different Rayleigh numbers ($10^3 \leq Ra \leq 10^6$).

In this case, there is hot bottom wall, linearly heated left side vertical wall, cold right side vertical wall and adiabatic top wall.

In this case, hot air leaves the hot bottom wall, moves upward along the linearly heated left side wall, reaches the top adiabatic wall and comes down along the cold right side wall forming a clockwise circulation in the cavity. Some secondary air circulations may be present at the left top corner.

4.2.2 Variation of Isotherms with Rayleigh Number

In the Fig. 13, isotherms are shown for the square cavities with the linearly heated left side wall and cold right side wall at different Rayleigh numbers ($10^3 \leq Ra \leq 10^6$).

In this case, isotherms are smooth curves at lower Rayleigh number ($Ra = 1.0 \times 10^3$). This indicates that the conduction and radiation dominate at the lower Rayleigh number.

At the higher Rayleigh number, isotherms are curved and pushed towards the top surface showing the increased buoyant force and dominance of convective heat transfer.

Due to the radiative heat transfer between the walls, the top adiabatic wall becomes heated. This shows that the temperature of colder parts of the cavity increases due to radiative interaction between the cavity walls.

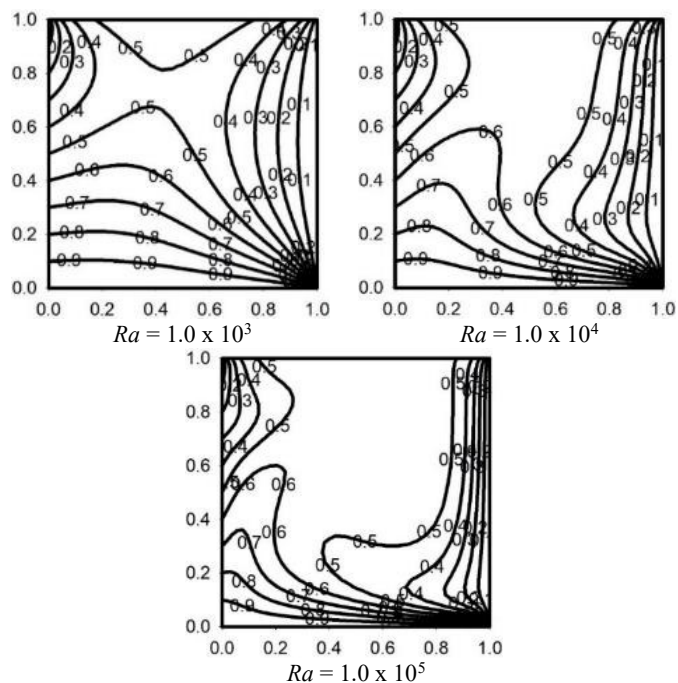


Fig. 13 Variation of isotherms with Rayleigh number (For $A = 1, N_{rc} = 42.261, Pr = 0.70, T_R = 0.854, \epsilon = 0.85$)

4.2.3 Variation of Local Nuc at Bottom Wall with Rayleigh Number

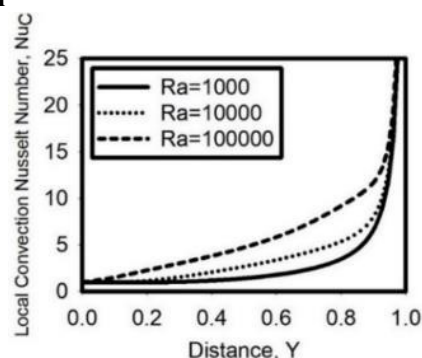


Fig. 14 Variation of local Nuc at bottom wall with Rayleigh number (For $A = 1, N_{rc} = 42.261, Pr = 0.70, T_R = 0.854, \epsilon = 0.85$)

Fig. 14 shows the variation of the local Nuc at the bottom wall with Rayleigh number. There at the left end, the local Nuc is equal to unity due to linearly heated left side wall and it is maximum near the cold right side wall. In all the cases, the local Nuc increases from left to right. With the increase in Rayleigh number, the strong air circulation formed increases the local Nuc at the bottom wall.

4.2.4 Variation of Local Nu_R at Bottom Wall with Rayleigh Number

Fig. 15 shows the variation of local Nu_R at the bottom wall with Rayleigh number. It is also observed that the local Nu_R at bottom wall increases from left to right. The reason attributed to the increased Nu_R at right is the presence of cold wall at the right side. The cold wall emits lesser irradiation, which results in lesser irradiation received by the walls near it and enhanced cooling of the bottom wall by the radiative heat transfer. It is observed that with the increase in Rayleigh number, the local Nu_R at bottom wall is slightly reduced.

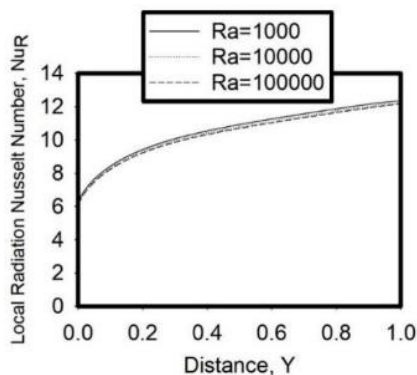


Fig. 15 Variation of local Nu_R at bottom wall with Rayleigh number (For $A = 1$, $N_{rc} = 42.261$, $Pr = 0.70$, $T_R = 0.854$, $\epsilon = 0.85$)

4.2.5 Variation of Local Nu_C at linearly heated left side wall with Rayleigh Number

Fig. 16 shows the variation of the local Nu_C at the linearly heated left side wall with Rayleigh number. The local Nu_C at the bottom of linearly heated left side wall is zero due to uniformly heated hot bottom wall and hot left side wall. It is maximum at the top edge near the adiabatic top wall. At the lower Rayleigh number ($Ra = 1.0 \times 10^3$), the local Nu_C is close to zero up to a distance $X = 0.6$ due to the weak air circulations. At the higher Rayleigh number, the local Nu_C increases due to increased air circulations. The fluctuations in local Nu_C at the linearly heated left side wall at higher Rayleigh number is a result of interaction between the downward primary and secondary air circulations with the linearly heated left side wall.

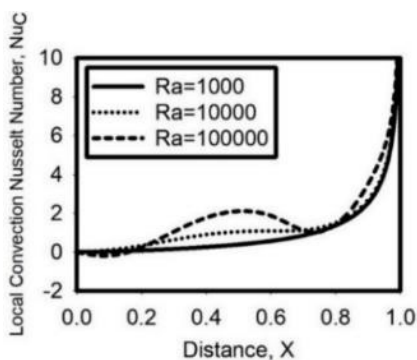


Fig. 16 Variation of local Nu_C at linearly heated left side wall (For $A = 1$, $N_{rc} = 42.261$, $Pr = 0.70$, $T_R = 0.854$, $\epsilon = 0.85$)

4.2.6 Variation of Local Nu_R at linearly heated left side wall with Rayleigh Number

Fig. 17 shows the variation of local Nu_R at the linearly heated left side wall with Rayleigh number. The local Nu_R is negative at the bottom of linearly heated left side wall, whereas it has a very high positive values near the top edge. The negative value of local Nu_R at the bottom shows that there the left wall is losing heat by the radiative heat transfer. The upper part of left wall has a positive Nu_R showing that there it is gaining

heat by the radiative heat transfer. Near the top edge, the left wall has a very high positive value of Nu_R due to presence of the adiabatic top wall close to it. It is observed that with the increase in Rayleigh number, the local Nu_R at bottom wall is slightly changed.

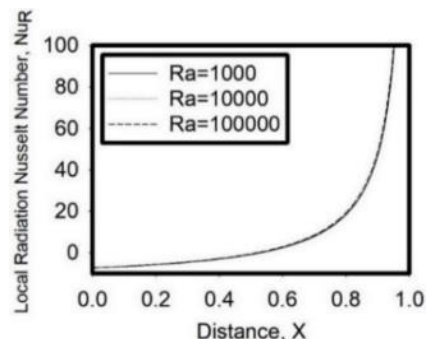


Fig. 17 Variation of local Nu_R at linearly heated left side wall (For $A = 1$, $N_{rc} = 42.261$, $Pr = 0.70$, $T_R = 0.854$, $\epsilon = 0.85$)

4.2.7 Variation of $\overline{Nu_C}$ and $\overline{Nu_R}$ at Bottom Wall with Surface Emissivity

Fig. 18 shows the variation of $\overline{Nu_C}$ and $\overline{Nu_R}$ at the bottom surface of cavity with the emissivity of cavity walls.

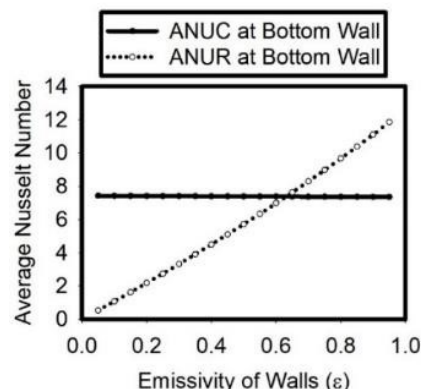


Fig. 18 Variation of $\overline{Nu_C}$ (ANUC) and $\overline{Nu_R}$ (ANUR) at bottom surface with surface emissivity (For $A = 1$, $N_{rc} = 42.261$, $Pr = 0.70$, $Ra = 7.0 \times 10^4$, $T_R = 0.854$)

It can be observed that the $\overline{Nu_C}$ is almost constant with increasing emissivity. This may be attributed to the fact that the emissivity of the side walls has a less significant effect on the cooling by air circulation inside the cavity.

The $\overline{Nu_R}$ at the bottom surface increases linearly with the emissivity of cavity walls. This may be attributed to the fact that radiative heat transfer between the walls is directly proportional to the emissivity of the cavity walls.

The $\overline{Nu_C}$ at the bottom wall in the cavity with only left side linearly heated wall is higher than in the case with both the left and right side linearly heated wall. This is due to better cooling of uniformly heated hot bottom wall in the cavity with only left side linearly heated wall due to the presence of a cold right side wall.

4.3 Comparison with results of Sathiyamoorthy *et al.* (2007b)

The results presented above is compared with the results of Sathiyamoorthy *et al.* (2007b).

In the present case, there is a significant thermal radiation heat transfer between the cavity walls even at the moderate emissivity. The formation of thermal boundary layer at the top adiabatic wall is a strong evidence of thermal radiation heat transfer between the cavity walls. In the results of the Sathiyamoorthy *et al.* (2007b), such thermal boundary layer is not observed in the absence of thermal radiation heat transfer.

Further, the increased temperature of top adiabatic wall due to thermal radiation heat transfer affects the natural convection inside the cavity. The top adiabatic wall gains heat from the other cavity walls through the thermal radiation heat transfer, which in turn loses heat to the air through the natural convection heat transfer. Thus, the thermal radiation heat transfer affects the streamlines and isotherms inside the cavity.

The effect of radiative heat transfer between the cavity walls on the streamlines is more prominent at the lower Rayleigh numbers. Here an increased value of the stream function indicates that the air circulation in the cavity becomes stronger due to radiative interaction between the cavity walls. It may give rise to some new minor air circulations at the left and right bottom corners of the cavity in the first case and at the left top corner of the cavity in the second case.

The radiative heat transfer between the cavity walls has significant effect on the isotherms inside the cavity. At the lower Rayleigh numbers in comparison with the Sathiyamoorthy *et al.* (2007b), the isotherms are shifted in the upward direction. This shows that the temperature of the major portion of the cavity is increased significantly. Most of the isotherms are bulged upwards at all the Rayleigh numbers. This may be attributed to the more heating of the top adiabatic wall by the radiative heat transfer.

It is also revealed that there is a significant change in local Nu_C due to radiative heat transfer between the cavity walls. The effect of radiative heat transfer between the cavity walls on the local Nu_C at the linearly heated vertical walls is greater near the top due to the presence of the top adiabatic wall. The effect of radiative heat transfer between the cavity walls on the local Nu_C at the bottom hot wall is less significant.

4.4 General Discussion

From the present study, the following observations are made.

1. In a closed cavity having linearly heated side walls, the fluid circulations primarily depend upon Rayleigh number.
2. At the lower Rayleigh number, the conduction and radiation are the dominant mode of heat transfer.
3. At the higher Rayleigh number, the primary air circulation becomes stronger. In this case, some small secondary air circulations may grow along with the strong primary air circulations enhancing the mixing of fluids.
4. At the higher Rayleigh number, the heat transfer by the natural convection increases in all the cases.
5. For the case of linearly heated left and right side walls:
 - (i.) The local Nu_C at the bottom wall is sinusoidal in nature with the minimum at the center.
 - (ii.) The local Nu_R at the bottom wall increases symmetrically from both the left and right side walls to the center and it is maximum at the midpoint.
 - (iii.) The local Nu_C at the linearly heated side wall is fluctuating in nature at the lower portion due to its interaction with the strong primary and secondary air circulation.
 - (iv.) The local Nu_C at the linearly heated side walls has a significantly increasing trend at its upper portion due to presence of top adiabatic wall close to it.
 - (v.) The local Nu_R at the linearly heated sidewall is negative at the points close to the bottom. It increases from bottom to top and it has a high positive value near the top adiabatic wall.
6. For the case of linearly heated left side wall and cold right side wall:
 - (i.) In this case, both the local Nu_C and local Nu_R at the bottom wall increases from left to right.
 - (ii.) The local Nu_C at the linearly heated left side wall shows a fluctuating behavior near the bottom due to its interaction with primary and secondary air circulations.
 - (iii.) The local Nu_R at the linearly heated left side wall is negative at the points close to bottom wall. It increases from bottom to top and it has a very high positive value near the top adiabatic wall.

7. The radiative heat transfer between the walls of the cavities affects the temperature of adiabatic wall and hence it affects the natural convection and streamlines in the cavities.
8. The radiative heat transfer increases the temperature of top adiabatic wall and at its vicinity and thus affects the isotherms inside the cavity.
9. Thus, the thermal radiation heat transfer affects the streamlines and isotherms inside the cavities in both the cases.
10. The local Nu_C at the bottom hot wall and left side linearly heated wall is not much affected by the emissivity of the walls in both the cases.
11. The local Nu_R at the bottom hot wall and left side linearly heated wall is proportional to the emissivity of the walls in both the cases.

The radiative heat transfer is comparable to convective heat transfer inside the cavity at the higher emissivity of the walls and hence neglecting the radiative heat transfer may produce erroneous results.

5. CONCLUSIONS

The thermal radiation heat transfer effects the temperature of the adiabatic walls. It causes more heating of the adiabatic walls even at the moderate emissivity. Thus, it affects the natural convection inside the cavity. It is reflected in the streamlines and isotherms inside the cavity. The surface radiation heat transfer cannot be neglected in comparison with the natural convection heat transfer. Therefore, neglecting the thermal radiation heat transfer may produce erroneous results.

NOMENCLATURE

A	aspect ratio (= H/d)
D	spacing between left and right walls, m
F_{ij}	shape factor between the elements i and j
g	acceleration due to gravity, 9.81 m.s ⁻²
G	dimensionless elemental irradiation
Gr_H	Grashof Number (based on H) = $g\beta(T_h - T_\infty)H^3/\nu^2$
H	height of the cavity, m
J	dimensionless elemental radiosity
m	total number of grid points in horizontal Y direction in the computational domain
n	total number of grid points in vertical X direction in the computational domain
N_{rc}	radiation-conduction parameter = $\sigma T_h^4/[k(T_h - T_\infty)/d]$
Nu_C	convection Nusselt number
$\overline{Nu_C}$	average convection Nusselt number
Nu_R	radiation Nusselt number
$\overline{Nu_R}$	average radiation Nusselt number
$\overline{Nu_T}$	sum of average convection Nusselt number and average radiation Nusselt number
Pr	Prandtl number
Ra_H	Rayleigh number (based on H) = $Gr_H.Pr$
T	temperature, K
T_x	temperature of left or right wall at a point having height x or having X-coordinate x, K
T_h	temperature of the hot wall of cavity, K
T_R	temperature ratio = T_∞ / T_h
T_∞	temperature of the ambient, K
U	dimensionless vertical velocity
V	dimensionless horizontal velocity
X	dimensionless vertical coordinate = x/d
Y	dimensionless horizontal coordinate = y/d

Greek Symbols

α	thermal diffusivity of fluid, m ² .s ⁻¹
β	isobaric co-efficient of volumetric thermal expansion of fluid, K ⁻¹
δ	convergence parameter in percentage = $\left (\zeta_{new} - \zeta_{old}) / \zeta_{new} \right \times 100$

ε	emissivity of the walls, dimensionless
ζ	symbol for the any dependent variable (ψ , ω , θ , J , G) over which convergence test is being applied
θ	dimensionless temperature = $(T - T_{\infty}) / (T_h - T_{\infty})$
ν	kinematic viscosity of the fluid, $m^2 \cdot s^{-1}$
σ	Stefan Boltzmann constant, $5.67 \times 10^{-8} \text{ W} \cdot m^{-2} \cdot K^{-4}$
ψ	dimensionless stream function
ω	dimensionless vorticity

Subscripts

c	cold
C	convection
h	hot
H	based on the height H of the left wall of closed cavity
i	any arbitrary elemental area of an enclosure in horizontal direction
j	any arbitrary elemental area of an enclosure in vertical direction
new	present value of any dependent variable (ψ , ω , θ , J , G) obtained in two successive iterations
old	previous value of any dependent variable (ψ , ω , θ , J , G) obtained in two successive iterations
rc	radiation-conduction
R	radiation
T	total
∞	ambient

REFERENCES

- Abdillah, H., and Novitrian, A., 2019, "Experiments on natural convection as cooling system mechanism on nuclear reactors," *Journal of Physics: Conference Series*, **1204**, 012111.
<https://dx.doi.org/10.1088/1742-6596/1204/1/012111>
- Al-Salem, K., Öztop, H.F., Pop, I., and Varol, Y., 2012, "Effects of moving lid direction on MHD mixed convection in a linearly heated cavity," *International Journal of Heat and Mass Transfer*, **55**(4), 1103-1112.
<https://dx.doi.org/10.1016/j.ijheatmasstransfer.2011.09.062>
- Balaji, C., and Venkateshan, S.P., 1994a, "Correlations for free convection and surface radiation in a square cavity," *International Journal of Heat and Fluid Flow*, **15**(3), 249-251.
[https://dx.doi.org/10.1016/0142-727X\(94\)90046-9](https://dx.doi.org/10.1016/0142-727X(94)90046-9)
- Balaji, C., and Venkateshan, S.P., 1994b, "Interaction of radiation with free convection in an open cavity," *International Journal of Heat and Fluid Flow*, **15**(4), 317-324.
[https://dx.doi.org/10.1016/0142-727X\(94\)90017-5](https://dx.doi.org/10.1016/0142-727X(94)90017-5)
- Basak, T., Roy, S., Sharma, P.K., and Pop, I., 2009a, "Analysis of mixed convection flows within a square cavity with linearly heated side wall(s)," *International Journal of Heat and Mass Transfer*, **52**(9-10), 2224-2242.
<https://dx.doi.org/10.1016/j.ijheatmasstransfer.2008.10.033>
- Basak, T., Roy, S., Singh, A., and Pandey, B.D., 2009b, "Natural convection flow simulation for various angles in a trapezoidal enclosure with linearly heated side wall(s)," *International Journal of Heat and Mass Transfer*, **52**(19-20), 4413-4425.
<https://dx.doi.org/10.1016/j.ijheatmasstransfer.2009.03.057>
- Basak, T., Roy, S., Singh, S.K., and Pop, I., 2010, "Analysis of mixed convection in a lid-driven porous square cavity with linearly heated side wall(s)," *International Journal of Heat and Mass Transfer*, **53**(9-10), 1819-1840.
<https://dx.doi.org/10.1016/j.ijheatmasstransfer.2010.01.007>
- Basak, T., Anandalakshmi, R., and Roy, M., 2013, "Heatlines based natural convection analysis in tilted isosceles triangular enclosures with linearly heated inclined walls: Effect of various orientations," *International Communications in Heat and Mass Transfer*, **43**, 39-45.
<https://dx.doi.org/10.1016/j.icheatmasstransfer.2013.01.008>
- Bouafia, M., and Daube, O., 2007, "Natural convection for large temperature gradients around a square solid body within a rectangular cavity," *International Journal of Heat and Mass Transfer*, **50**(17-18), 3599-3615.
<https://dx.doi.org/10.1016/j.ijheatmasstransfer.2006.05.013>
- Chaabane, R., 2019, "Free convection in a MHD open cavity with a linearly heated wall using LBM," In: Rojas, N.O. (Editor), *Pattern Formation and Stability in Magnetic Colloids*, IntechOpen, London.
<https://dx.doi.org/10.5772/intechopen.81177>
- Hasan, M.N., Saha, S.C., and Gu, Y.T., 2012, "Unsteady natural convection within a differentially heated enclosure of sinusoidal corrugated side walls," *International Journal of Heat and Mass Transfer*, **55**(21-22), 5696-5708.
<https://dx.doi.org/10.1016/j.ijheatmasstransfer.2012.05.065>
- Jones, A.T., and Ingham, D.B., 1993, "Combined convection flow in a vertical duct with wall temperatures that vary linearly with depth," *International Journal of Heat and Fluid Flow*, **14**(1), 37-47.
[https://dx.doi.org/10.1016/0142-727X\(93\)90038-0](https://dx.doi.org/10.1016/0142-727X(93)90038-0)
- Karatas, H., and Derbentli, T., 2018, "Natural convection and radiation in rectangular cavities with one active vertical wall," *International Journal of Thermal Sciences*, **123**, 129-139.
<https://dx.doi.org/10.1016/j.ijthermalsci.2017.09.006>
- Kefayati, G.R., Gorji-Bandpy, M., Sajjadi, H., and Ganji, D.D., 2012, "Lattice Boltzmann simulation of MHD mixed convection in a lid-driven square cavity with linearly heated wall," *Scientia Iranica*, **19**(4), 1053-1065.
<https://dx.doi.org/10.1016/j.scient.2012.06.015>
- Kefayati, G.H.R., 2014, "Natural convection of ferrofluid in a linearly heated cavity utilizing LBM," *Journal of Molecular Liquids*, **191**, 1-9.
<https://dx.doi.org/10.1016/j.molliq.2013.11.021>
- Kiran, S., Sankar, M., Gangadharaiyah, Y.H., and Dhananjayamurthy, B.V., 2021, "Natural convection in a linearly heated vertical porous annulus under the effect of magnetic field," In: Manik, G., Kalia, S., Sahoo, S.K., Sharma, T.K., and Verma, O.P. (Editors), *Advances in Mechanical Engineering*, Lecture Notes in Mechanical Engineering, Springer, Singapore, 537-546.
https://dx.doi.org/10.1007/978-981-16-0942-8_50
- Kumar, R.A., and Kunjunni, M., 2021, "Effect of linearly varying heating inside a square cavity under natural convection," *Journal of Applied research and Technology*, **19**(4), 336-344.
<https://dx.doi.org/10.22201/icat.24486736e.2021.19.4.1573>
- Mahmoodi, M., Arani, A.A.A., Sebdani, S.M., and Tajik, P., 2017, "Natural convection in nanofluid-filled square chambers subjected to linear heating on both sides: a numerical study," *Heat Transfer Research*, **48**(9), 771-785.
<https://dx.doi.org/10.1615/HeatTransRes.2016011010>
- Mliki, B., Ali, C., and Abbassi, M.A., 2020, "Lattice Boltzmann simulation of MHD natural convection heat transfer of Cu-water nanofluid in a linearly/sinusoidally heated cavity," *International Journal of Physical and Mathematical Sciences*, **14**(1), 11-17.
<https://dx.doi.org/10.5281/zenodo.3669174>

Natarajan, E., Basak, T., and Roy, S., 2007, "Natural convection in a trapezoidal cavity with linearly heated side wall(s)," *Proceedings of the ASME/JSME 2007 Thermal Engineering Heat Transfer Summer Conference collocated with the ASME 2007 InterPACK Conference. ASME/JSME 2007 Thermal Engineering Heat Transfer Summer Conference, Volume 1*, Vancouver, British Columbia, Canada, July 8–12, 2007, ASME, **1**, 1021-1030.
<https://dx.doi.org/10.1115/HT2007-32180>

Ostrach, S., 1954, "Combined natural and forced convection laminar flow and heat transfer of fluids with and without heat sources in channels with linearly varying wall temperatures," *National Advisory Committee for Aeronautics*, Technical Note **3141**, 1-74.
https://digital.library.unt.edu/ark:/67531/metadc56936/m2/1/high_res_d/19930083805.pdf
(Last accessed on 14th April, 2022)

Prasad, R.S., Singh, S.N., and Gupta, A.K., 2018a, "A systematic approach for optimal positioning of heated side walls in a side vented open cavity under natural convection and surface radiation," *Frontiers in Heat and Mass Transfer*, **11**, 15.
<https://dx.doi.org/10.5098/hmt.11.15>

Prasad, R.S., Singh, S.N., and Gupta, A.K., 2018b, "Coupled laminar natural convection and surface radiation in partially right side open cavities," *Frontiers in Heat and Mass Transfer*, **11**, 28.
<https://dx.doi.org/10.5098/hmt.11.28>

Prasad, R.S., Singh, S.N., and Gupta, A.K., 2019, "Combined laminar natural convection and surface radiation in top open cavities with right side opening," *Journal of Engineering Science and Technology*, **14**(1), 387-410.
https://jestec.taylors.edu.my/Vol%2014%20Issue%201%20February%202019/14_1_27.pdf
(Last accessed on 14th April, 2022)

Prasad, R.S., Nayak, U.K., Nayak, R.K., and Gupta, A.K., 2022, "Combined natural convection and surface radiation in a square cavity with the inversely linearly heated opposite side walls," *Frontiers in Heat and Mass Transfer*, **19**, 4.
<https://dx.doi.org/10.5098/hmt.19.4>

Prud'homme, M., and Bougherara, H., 2005, "Weakly non-linear stability of stratified natural convection in a vertical cavity with lateral temperature gradient," *International Communications in Heat and Mass Transfer*, **32**(1–2), 32–42.
<https://dx.doi.org/10.1016/j.icheatmasstransfer.2004.02.020>

Şahin, B., 2020, "Effects of the center of linear heating position on natural convection and entropy generation in a linearly heated square cavity," *International Communications in Heat and Mass Transfer*, **117**, 104675.
<https://dx.doi.org/10.1016/j.icheatmasstransfer.2020.104675>

Sankar, M., Kiran, S., and Sivasankaran, S., 2018, "Natural convection in a linearly heated vertical porous annulus," *Journal of Physics: Conference Series*, **1139**, 012018.
<https://dx.doi.org/10.1088/1742-6596/1139/1/012018>

Saravanan, S., and Sivaraj, C., 2015, "Combined natural convection and thermal radiation in a square cavity with a non-uniformly heated plate," *Computers & Fluids*, **117**, 125–138.
<https://dx.doi.org/10.1016/j.compfluid.2015.05.005>

Sathiyamoorthy, M., Basak, T., Roy, S., and Mahanti, N.C., 2007a, "Effect of the temperature difference aspect ratio on natural convection in a square cavity for nonuniform thermal boundary conditions," *Journal of Heat Transfer*, **129**(12), 1723-1728.
<https://dx.doi.org/10.1115/1.2768099>

Sathiyamoorthy, M., Basak, T., Roy, S., and Pop, I., 2007b, "Steady natural convection flows in a square cavity with linearly heated side wall(s)," *International Journal of Heat and Mass Transfer*, **50**(3–4), 766–775.
<https://dx.doi.org/10.1016/j.ijheatmasstransfer.2006.06.019>

Sathiyamoorthy, M., Basak, T., Roy, S., and Pop, I., 2007c, "Steady natural convection flow in a square cavity filled with a porous medium for linearly heated side wall(s)," *International Journal of Heat and Mass Transfer*, **50**(9–10), 1892-1901.
<https://dx.doi.org/10.1016/j.ijheatmasstransfer.2006.10.010>

Sathiyamoorthy, M., and Chamkha, A., 2010, "Effect of magnetic field on natural convection flow in a liquid gallium filled square cavity for linearly heated side wall(s)," *International Journal of Thermal Sciences*, **49**(9), 1856-1865.
<https://dx.doi.org/10.1016/j.ijthermalsci.2010.04.014>

Sathiyamoorthy, M., and Chamkha, A.J., 2012, "Natural convection flow under magnetic field in a square cavity for uniformly (or) linearly heated adjacent walls," *International Journal of Numerical Methods for Heat & Fluid Flow*, **22**(5), 677-698.
<https://dx.doi.org/10.1108/09615531211231307>

Singh, S.N., and Venkateshan, S.P., 2004, "Numerical study of natural convection with surface radiation in side-vented open cavities," *International Journal of Thermal Sciences*, **43**(9), 865–876.
<https://dx.doi.org/10.1016/j.ijthermalsci.2004.01.002>

Singh, D.K., and Singh, S.N., 2015, "Conjugate free convection with surface radiation in open top cavity," *International Journal of Heat and Mass Transfer*, **89**, 444-453.
<https://dx.doi.org/10.1016/j.ijheatmasstransfer.2015.05.038>